IEEE Access
Multidisciplinary | Rapid Review | Open Access Journal

Received April 7, 2022, accepted April 22, 2022, date of publication May 2, 2022, date of current version May 16, 2022.

Digital Object Identifier 10.1109/ACCESS.2022.3171564

Multiobjective Heterogeneous Asymmetric Sliding Mode Control of Nonlinear Connected Autonomous Vehicles

YAN YAN[1], (Student Member, IEEE), HAIPING DU[1], (Senior Member, IEEE), YAFEI WANG[2], (Member, IEEE), AND WEIHUA LI[1], (Senior Member, IEEE)

[1]School of Electrical, Computer and Telecommunications Engineering, University of Wollongong, Wollongong, NSW 2522, Australia
[2]School of Mechanical Engineering, Shanghai Jiao Tong University, Shanghai 200240, China

Corresponding author: Yan Yan (yy436@uowmail.edu.au)

This work was supported by the Australian Research Council's Discovery Projects Funding Scheme under Grant DP:200100149.

ABSTRACT Platoon of connected autonomous vehicles has the potential to increase traffic flow while also alleviating congestion. However, there are several challenging problems with heterogeneous connected autonomous vehicles control currently. Platoons with heterogeneous vehicles are especially susceptible to the negative effects of wireless communication. A multi-objective heterogeneous asymmetric sliding mode control strategy is proposed in this paper to solve this problem. In this paper, a nonlinear vehicle dynamic model is considered. Then, a sliding mode controller is designed to achieve consensus. Moreover, Riccati inequality and Lyapunov analysis are used to find the controller's gains and guarantee Lyapunov stability and string stability with the linear matrix inequalities. Finally, a non-dominated sorting genetic algorithm II is utilized to find the Pareto optimal heterogeneous asymmetric degrees regarding the overall performance of the platoon, including tracking index, fuel consumption and acceleration standard deviation. The results show that the proposed strategy can effectively deal with platoons of heterogeneous vehicles while ensuring stability. At the same time, Pareto optimal heterogeneous asymmetric degrees can be obtained for each vehicle in the platoon. The proposed method improves platoon's tracking ability by 76.2%, fuel economy by 3.53% and driving comfort by 3.52%.

INDEX TERMS Asymmetric degrees, CAV, nonlinear vehicular platoon, NSGA-II, sliding mode control.

I. INTRODUCTION

Connected autonomous vehicles (CAVs) have been identified as a critical aspect of the intelligent transportation system. The platoon of CAVs is gaining popularity due to its practical value [1]. Platoon control is the process of controlling a group of CAVs to an ideal steady state. The following vehicles track the leading vehicles with a desirable velocity while maintaining a safe and comfortable inter-vehicle gap [2]. Platoon control methods have a number of recognized benefits, including improved traffic mobility, safety, and emission reduction [3]. According to research, improving the aerodynamics of vehicle platoons will result in a 6% -10% increase in fuel economy [4]. Moreover, platoon modelling, control architecture, and performance requirements are regarded as the three most critical aspects of platoon [1].

The associate editor coordinating the review of this manuscript and approving it for publication was Razi Iqbal.

Platoon modelling is primarily concerned with two aspects: the vehicle dynamic model and the information flow topology. In the state-of-the-art [5]–[7], a class of linearized third-order vehicle dynamic model is considered in the control problem. Our previous work [8] also considered a linear model for vehicle dynamics with an exact feedback linearisation technique. However, it is based on the assumption that all vehicular parameters are precisely known, which is not realistic in reality. Therefore, several studies considered a nonlinear vehicle dynamic model to reflect the control problem more accurately. For example, Feng *et al.* [9] presented a distributed coordinated controller for nonlinear vehicle dynamic model in both lateral and longitudinal motions. It includes an online estimate of unknown parameters and disturbances. To deal with topological uncertainty, a decoupling approach based on topological matrix's eigenvalue decomposition and linear transformation is also proposed. In order to address the control problem more precisely,

this paper considers a third-order nonlinear vehicle dynamic model.

The information flow topology is also important in the platoon modelling. It explains the connectivity relations between connected vehicles. Our previous work [10] confirms that different types of information flow topologies have a significant impact on the performance of CAVs. Different topologies also result in distinct topological matrices, where the eigenvalues are critical for determining the platoon's stability and string stability. The variety of information flow topology naturally introduces new challenges to CAVs platoon control [4]. In the state-of-the-art [11]–[14], symmetric information flow topologies are considered in almost all control problems, however, due to the uncertainty of wireless communication, it is neither practical nor efficient. On the other hand, the benefits of implementing asymmetric information flow topology have gained interest in recent years. It has been observed that asymmetric information flow topology can predominantly benefit platooning of connected autonomous vehicles by mitigating the negative effect of wireless communication [15]–[17]. Zheng *et al.* [15] offered some insight upon this subject. The study demonstrated that one of the most important benefits of implementing asymmetric control is that the stability margin for particular topologies can be independent of platoon size while bounded away from zero. As a result, with asymmetric control, a scalable platoon with a constant stability margin can be obtained. Herman *et al.* [16] discovered a similar regularity. The research studied the asymmetry of inter-vehicular coupling using asymmetric bidirectional platoon control. The results indicated that even if the harmonic instability exists for linear controllers, the Laplacian eigenvalues can still be bounded, which showed great advantages. Herman and Sebek [17] also created a LQR optimal distributed controller to optimise the feedback gains in an asymmetric topology. The strategy was shown to be useful beyond the platoon scale. However, as the scaling grew exponentially and became dependent on the controller's tuning, a barrier was formed. However, these research studied a single asymmetric degree. Not only is this approach impractical for heterogeneous platoons, but it also falls short of completely exploiting the benefits of asymmetric control. Most of the previous studies selected asymmetric degrees arbitrarily and artificially [15]–[16], and there was insufficient information on how to select an asymmetric degree. Our previous study [8] proposed a strategy to find an optimal asymmetric degree in the platoon, based on our previous work [8], this study aims to solve a more complex control problem while making full use of asymmetric control by finding heterogeneous asymmetric agrees with an optimisation purpose.

The control architecture of platoon has been studied intensively in the past decades. Among all control strategies, the sliding mode control strategy stands out due to promising ability to handle nonlinear dynamics, actuator constraints and information flow topology diversity [1]. Guo *et al.* [18] developed a method for adaptive fuzzy sliding mode control of longitudinal and lateral vehicle dynamics in a platoon. The system's asymptotic stability was established using the Lyapunov stability principle. The approach has been shown to be extremely beneficial in dealing with nonlinearity and external disturbances. To cope with unknown driving resistance and actuator saturation, Song and Ju [19] developed a distributed adaptive sliding mode control algorithm. An adaptive updating law was included, as well as an anti-windup compensation-based approach. As a result, the unknown driving coefficients can be determined, and the platoon's integral windup can be reduced. Guo and Li [20] developed a set-point optimisation layer and a vehicle tracking control layer to address the issue of fuel-time efficient platooning control. The optimum speed of the vehicles was determined using a speed-planning algorithm, while the sliding mode controller ensures string stability. The methodology also examined the fuel economy of road freight transport vehicles. However, one of the most critical issues is determining the sliding mode controller's gains. The majority of methods [20]–[22] guaranteed string stability using a basic control mechanism, such as the transfer function method, which allows for a broad variety of possible controller's gains. The controller's gains were then arbitrarily chosen within a broad range, ignoring theoretical justification and infusing the control system with randomness. Therefore, this paper fills the void by using a Riccati inequality to determine the feasible controller's gains. The Routh-Hurwitz criterion is also used to guarantee the control system's asymptotical stability.

Performance evaluation is another critical part of platoon control objectives. Historically, model predictive controllers (MPC) were often used to address a variety of control objectives. It can optimise platoon trajectories by addressing constrained issues [23]. Weighted sum is a technique that is often used in the construction of optimisation functions. Fixed weighting factors are prefered in certain studies. Yang *et al.* [24] established a model for eco-driving platoon control that prioritises journey duration, fuel consumption, and safety. The suggested approach, which incorporates two-stage control logic and an integrated traffic flow model, has the potential to reduce highway congestion while also lowering fuel usage. Additionally, it emphasizes that choosing weighting coefficients requires a trade-off between several objectives, and hence that optimisation techniques with constrained weighting coefficient combinations are not practical. Using fixed weighting coefficients has drawbacks [25], since the best solution is typically the corner solution on the Pareto front, and it also changes drastically when the weighting factors are altered substantially. Numerous research employed a weighting coefficient tuning strategy to avoid these restrictions. Yu *et al.* [26] used an MPC controller to design a dynamic weight tuning optimisation technique for increasing trip comfort and minimising tracking error. According to the study, it outperformed the conventional methods. Zhao *et al.* [27] developed a comparable real-time weight tuning mechanism. Due to the fact that the weighting coefficients in all trials are highly reliant on the inter-vehicle states, any feedback delay has the potential to significantly

weaken platoon stability. To address the limitations of the state-of-the-art [23]–[27], this work offers the NSGA-II algorithm for optimising platoon performance, including tracking capability, fuel efficiency, and drive comfort. Utilizing an evolutionary algorithm allows for the preservation of a collection of outstanding Pareto optimum solutions while avoiding all of the above shortcomings.

Overall, this paper presents a study on the multi-objective sliding mode control of CAVs with heterogeneous asymmetric degrees for each vehicle. The sliding mode controller's gains and the heterogeneous asymmetric degrees will be optimally determined using the LMIs and learning algorithm's feasible solutions. In our previous work [8], we proposed an asymmetric sliding mode controller for optimising platoon performance with multiple objectives. This research builds on our previous work [8], but employs a more advanced controller design to address a more complex control problem. To begin, a nonlinear vehicle dynamic model is considered. Following that, a more advanced nonlinear sliding mode controller is presented. Finally, searching for heterogeneous asymmetric degrees in a heterogenous platoon complicates the control problem. The main contributions of this paper are:

(i) In the context of choosing the sliding mode controller's gains, the past studies selected the controller's gains arbitrarily within a wide range determined by simple methods [15], [20], [22], such as the transfer function method. However, this study employs a Riccati inequality based sliding mode control strategy to calculate the feasible controller's gains. As a result, A closed-loop stability theorem for a nonlinear heterogeneous platoon interconnected by the asymmetric topologies is derived using the Lyapunov analysis.

(ii) The state-of-the-art [23]–[27] have lots of shortcomings when applied to platoon's multi-objective optimisation. To bridge the gaps, this paper suggests NSGA-II algorithm. It overcomes the sensitivity and optimality issues that arise from the restricted number of fixed weighting coefficient alternatives. This study is able to acquire the whole Pareto front by generating a large number of Pareto optimum solutions. It can balance trade-offs and delivers flexible optimum solutions that adapt to the platoon's priorities under varying circumstances.

(iii) In the context of asymmetric control, the past studies selected and considered one asymmetric degree randomly [15], [16]. This study further proposes a strategy to find the Pareto optimal heterogeneous asymmetric degrees in the topological matrix to achieve multiple objectives. It is demonstrated that the optimal heterogeneous asymmetric degrees can enhance the platoon's overall performance.

(iv) Extensive simulations and analyses are performed to validate the effectiveness of the proposed control method. The Urban Road Case Study and the Highway Case Study are both taken into account. Under both case studies, three traditional information flow topologies and one random information flow topology constructed based on the packet drop rate are all tested. As a result, the efficacy of the proposed strategy is proved.

The remainder of the paper is organized as follows: Section II presents the problem statement. Section III describes the design of the sliding mode controller. Section IV presents the proposed multi-objective heterogeneous asymmetric degrees optimisation strategy. Simulation and results are discussed in Section V. Section VI gives conclusions and future recommendations.

II. PROBLEM STATEMENT

The platoon discussed in this study has N+1 vehicles, including one leading vehicle and N following vehicles. The section consists of three main components: 1) Vehicle dynamic model; 2) Information flow topology; 3) Heterogeneous asymmetric degrees. Each vehicle's dynamic behavior is described by the vehicle dynamic model. The information flow topology depicts how vehicles communicate with one another. Finally, heterogeneous asymmetric degrees are used to characterize the intensity of connectivity between heterogeneous vehicles. It is incorporated into the model through the modification of the topological matrix.

A. VEHICLE DYNAMICS MODEL

Applying the leader-follower approach, we consider the leader of the system as [28]:

$$\begin{aligned} \dot{p}_0(t) &= v_0(t) \\ \dot{v}_0(t) &= a_0(t) \end{aligned} \tag{1}$$

where $p_0(t)$, $v_0(t)$ and $a_0(t)$ are the longitudinal position, velocity and acceleration of the leader vehicle. We consider the model for vehicle i as [2]:

$$\begin{aligned} \dot{p}_i(t) &= v_i(t) \\ \dot{v}_i(t) &= a_i(t) \\ \dot{a}_i(t) &= -\frac{a_i(t)}{\tau_i} + \frac{u_i(t)}{m_i\tau_i} - \frac{2K_{di}v_i(t)\,a_i(t)}{m_i} - \frac{K_{di}v_i(t)^2}{m_i\tau_i} \\ &\quad - \frac{d_{mi}}{m_i\tau_i} \end{aligned} \tag{2}$$

where $p_i(t)$, $v_i(t)$ and $a_i(t)$ are the longitudinal position, velocity and acceleration of vehicle i. $u_i(t)$ is the control input of vehicle i. m_i(kg) is the vehicle mass, τ_i (s) is the vehicle engine time, K_{di} is the vehicle aerodynamic drag coefficient, d_{mi} (N) is the mechanical drag. This study takes into account a platoon of heterogeneous vehicles, which means that each vehicle has heterogeneous vehicle dynamics properties in terms of the aforementioned parameters. Specific values for each vehicle's dynamics parameters are chosen at random within a reasonable range and are displayed in Table 1. To simplify the presentation, (2) can be rewritten as:

$$\dot{a}_i(t) = -\frac{a_i(t)}{\tau_i} + \frac{u_i(t)}{m_i\tau_i} - \theta^T\omega$$

FIGURE 1. TPSF topology.

where

$$\theta = \begin{bmatrix} \frac{2K_{di}}{m_i} \\ \frac{K_{di}}{m_i\tau_i} \\ \frac{d_{mi}}{m_i\tau_i} \end{bmatrix}, \quad \omega = \begin{bmatrix} v_i(t)a_i(t) \\ v_i(t)^2 \\ 1 \end{bmatrix} \tag{3}$$

B. INFORMATION FLOW TOPOLOGY MODEL

The topology discussed in this study is two predecessors single following topology (TPSF). It is selected based on its bidirectional complexity that allows the opportunity to investigate the impact of wireless communication fully. TPSF topology is shown in Fig.1 below.

In Fig.1, each vertex represents a CAV and each edge represents an active communication link. Information each CAV can send and receive information includes position, velocity and acceleration in both longitudinal and lateral directions.

The mathematical description of the connection of topology can be defined as [1]: $G = \{V, E, T\}$ where G is a weighted graph of order N consists of 3 elements: V represents the set of N nodes, $E \subseteq V \times V$ denotes the set of edges, which is also the communication link between vehicles; $T = [t_{ij}]$ represents the adjacency matrix of G. If there is a communication link from agent j to agent i, which means agent i can receive information from agent j, $t_{ij} = 1$, otherwise $t_{ij} = 0$. The in-degree of node i is defined as $d_i = \sum_{j=1}^{N} t_{ij}$. Denote $D = diag\,(d_1, d_2 \ldots d_N)$, the Laplacian matrix L is defined as $L = D - T$.

Considering N followers and one leader in the weighted graph G, we define $P = diag(p_1, p_2 \ldots p_N)$ as the linked matrix of G, where if agent i receives information from the leader, $p_i = 1$, otherwise $p_i = 0$.Then the overall topological matrix in this study is represented by $H = L + P$.

Taking the symmetric TPSF topology as an example, for a platoon with one leader and five followers, the adjacency matrix T is:

$$\begin{bmatrix} 0 & 1 & 0 & 0 & 0 \\ 1 & 0 & 1 & 0 & 0 \\ 1 & 1 & 0 & 1 & 0 \\ 0 & 1 & 1 & 0 & 1 \\ 0 & 0 & 1 & 1 & 0 \end{bmatrix}$$

$D = diag\,(1, 2, 3, 3, 2)$. Therefore the Laplacian matrix L is:

$$\begin{bmatrix} 1 & -1 & 0 & 0 & 0 \\ -1 & 2 & -1 & 0 & 0 \\ -1 & -1 & 3 & -1 & 0 \\ 0 & -1 & -1 & 3 & -1 \\ 0 & 0 & -1 & -1 & 2 \end{bmatrix}$$

The linked matrix $P = diag(1, 1, 0, 0, 0)$. The overall topological matrix H is:

$$\begin{bmatrix} 2 & -1 & 0 & 0 & 0 \\ -1 & 3 & -1 & 0 & 0 \\ -1 & -1 & 3 & -1 & 0 \\ 0 & -1 & -1 & 3 & -1 \\ 0 & 0 & -1 & -1 & 2 \end{bmatrix}$$

In addition, we define a neighbour set of node i in the following as:

$$\mathbb{N}_i = \{j \epsilon V | t_{ij} = 1\}$$

The leader accessible set of node i is defined as

$$\mathbb{R}_i = \begin{cases} \{0\} & if\ p_i = 1 \\ \emptyset & if\ p_i = 0 \end{cases}$$

Therefore, the complete topology information set of node i is defined as

$$\Pi_i = \mathbb{N}_i \cup \mathbb{R}_i$$

C. HETEROGENEOUS ASYMMETRIC DEGREES MODEL

Referring to [15], heterogeneous asymmetric degrees ε_i are introduced in the system, where $0 < \varepsilon_i < 1$. When vehicle i receives information from the vehicles ahead of it, the communications are regarded as more reliable, therefore the communication links are enhanced by ε_i, and vice versa. When $\varepsilon_i = 0$, the system becomes symmetric.

Here is the process of incorporating heterogeneous asymmetric degrees ε_i into the topological matrix. Firstly the adjacency matrix T is separated into T_1 and T_2,where T_1 is an upper triangular matrix and T_2 is a lower triangular matrix. If $j < i$, the communication link is denoted by an adjacency matrix T_1, if $j > i$, the communication link is denoted by an adjacency matrix T_2.

Then, heterogeneous asymmetric degrees ε_i are introduced to the adjacency matrix T:

$$t_{ij} = \begin{cases} 1 + \varepsilon_i & if\ t_{ij} = 1\ \ and\ \ t_{ij} \in T_1 \\ 1 - \varepsilon_i & if\ t_{ij} = 1\ \ and\ \ t_{ij} \in T_2 \end{cases}$$

By enforcing heterogeneous asymmetric degrees ε_i, with the same example mentioned above, T_1 and T_2 can be obtained as:

$$T_1 = \begin{bmatrix} 0 & 0 & 0 & 0 & 0 \\ 1+\varepsilon_2 & 0 & 0 & 0 & 0 \\ 1+\varepsilon_3 & 1+\varepsilon_3 & 0 & 0 & 0 \\ 0 & 1+\varepsilon_4 & 1+\varepsilon_4 & 0 & 0 \\ 0 & 0 & 1+\varepsilon_5 & 1+\varepsilon_5 & 0 \end{bmatrix},$$

$$T_2 = \begin{bmatrix} 0 & 1-\varepsilon_1 & 0 & 0 & 0 \\ 0 & 0 & 1-\varepsilon_2 & 0 & 0 \\ 0 & 0 & 0 & 1-\varepsilon_3 & 0 \\ 0 & 0 & 0 & 0 & 1-\varepsilon_4 \\ 0 & 0 & 0 & 0 & 0 \end{bmatrix},$$

$$T_\varepsilon = \begin{bmatrix} 0 & 1-\varepsilon_1 & 0 & 0 & 0 \\ 1+\varepsilon_2 & 0 & 1-\varepsilon_2 & 0 & 0 \\ 1+\varepsilon_2 & 1+\varepsilon_3 & 0 & 1-\varepsilon_3 & 0 \\ 0 & 1+\varepsilon_4 & 1+\varepsilon_4 & 0 & 1-\varepsilon_4 \\ 0 & 0 & 1+\varepsilon_5 & 1+\varepsilon_5 & 0 \end{bmatrix}.$$

where T_ε is the adjacency matrix with heterogeneous asymmetric degrees. It can be seen that $T_\varepsilon = T_1 + T_2$. Therefore D_ε can also be separated into D_1 and D_2 corresponding to T_1 and T_2.

$$D_1 = diag\,(0, 1+\varepsilon_2, 2+2\varepsilon_3, 2+2\varepsilon_4, 2+2\varepsilon_5),$$
$$D_2 = diag\,(1-\varepsilon_1, 1-\varepsilon_2, 1-\varepsilon_3, 1-\varepsilon_4, 0),$$
$$D_\varepsilon = D_1 + D_2 = diag\,(1-\varepsilon_1, 2, 3+\varepsilon_3, 3+\varepsilon_4, 2+2\varepsilon_5).$$

The linked matrix with the asymmetric degree is P_ε, $P_\varepsilon = diag(1+\varepsilon_1, 1+\varepsilon_2, 0, 0, 0)$.

By introducing heterogeneous asymmetric degrees, the Laplacian matrix becomes L_ε and topological matrix becomes H_ε.

$$L_\varepsilon = \begin{bmatrix} 1-\varepsilon_1 & -1+\varepsilon_1 & 0 & 0 & 0 \\ -1-\varepsilon_2 & 2 & -1+\varepsilon_2 & 0 & 0 \\ -1-\varepsilon_3 & -1-\varepsilon_3 & 3+\varepsilon_3 & -1+\varepsilon_3 & 0 \\ 0 & -1-\varepsilon_4 & -1-\varepsilon_4 & 3+\varepsilon_4 & -1+\varepsilon_4 \\ 0 & 0 & -1-\varepsilon_5 & -1-\varepsilon_5 & 2+2\varepsilon_5 \end{bmatrix},$$

$$H_\varepsilon = \begin{bmatrix} 2 & -1+\varepsilon_1 & 0 & 0 & 0 \\ -1-\varepsilon_2 & 3+\varepsilon_2 & -1+\varepsilon_2 & 0 & 0 \\ -1-\varepsilon_3 & -1-\varepsilon_3 & 3+\varepsilon_3 & -1+\varepsilon_3 & 0 \\ 0 & -1-\varepsilon_4 & -1-\varepsilon_4 & 3+\varepsilon_4 & -1+\varepsilon_4 \\ 0 & 0 & -1-\varepsilon_5 & -1-\varepsilon_5 & 2+2\varepsilon_5 \end{bmatrix}.$$

The neighbour sets of node i are divided into two sets, $\mathbb{N}_{i_1}$ and $\mathbb{N}_{i_2}$, which is defined as:

$$\mathbb{N}_{i_1} = \{j \epsilon V | t_{ij} = 1+\varepsilon_i, t_{ij} \in T_1\}$$
$$\mathbb{N}_{i_2} = \{j \epsilon V | t_{ij} = 1-\varepsilon_i, t_{ij} \in T_2\}$$

The leader accessible set of node i is defined as

$$\mathbb{R}_i = \begin{cases} \{0\} & if\ p_i = 1+\varepsilon_i \\ \emptyset & if\ p_i = 0 \end{cases}$$

Therefore, the topology information sets of node i are also divided into two sections, which are defined as

$$\Pi_{i_1} = \mathbb{N}_{i_1} \cup \mathbb{R}_i$$
$$\Pi_{i_2} = \mathbb{N}_{i_2}$$
$$\Pi_i = \Pi_{i_1} \cup \Pi_{i_2}$$

After introducing heterogeneous asymmetric degrees ε_i into the topological matrix, H_ε will be used in the following sections when referring to the complete topology information set Π_i. Among all the vehicles that vehicle i receives information from, the first topology information set Π_{i_1} refers to the vehicles ahead of vehicle i, including the leader. The second topology information set Π_{i_2} refers to vehicles behind vehicle i. The maximum and minimum eigenvalues of a certain type of topology are expressed as $\lambda_{max}(H_\varepsilon)$ and $\lambda_{min}(H_\varepsilon)$ respectively. It is assumed that all topologies discussed in this study are positive definite [29].

Notations: $\mathbb{R}^n$ is the n-dimensional Euclidean space. $\|\ .\ \|_{l_2}$ is the l_2-norm. $\lambda\ (A)$ represents the eigenvalue of Matrix A. 1_N is a column vector of size N with all its entries being 1. $\otimes$ is the Kronecker product.

III. SLIDING MODE CONTROLLER DESIGN

A. SLIDING MODE CONTROLLER

Heterogeneous asymmetric degrees sliding mode controller is proposed in this section as follows. The tracking error with asymmetric degree was discussed in our previous work [8], therefore, the sliding surface is selected to be:

$$\begin{aligned} s_i\,(t) = a_i\,(t) &+ (1+\varepsilon_i)\,k_1 \sum_{j \epsilon \Pi_{i_1}} p_i(t) - p_j(t) - d_{ij} \\ &+ (1-\varepsilon_i)\,k_1 \sum_{j \epsilon \Pi_{i_2}} p_i(t) - p_j(t) - d_{ij} \\ &+ (1+\varepsilon_i)\,k_2 \sum_{j \epsilon \Pi_{i_1}} v_i\,(t) - v_j\,(t) \\ &+ (1-\varepsilon_i) k_2 \sum_{j \epsilon \Pi_{i_2}} v_i(t) - v_j(t) \end{aligned} \tag{4}$$

where $k_1, k_2 > 0$, and they are controller's gain, Π_{i_1} and Π_{i_2} are complete topology information sets of node i stated in Section II. d_{ij} is the desired spacing between vehicle i and vehicle j, a predefined nonzero constant specified in Table 2.

Considering the convergence of the spacing error and velocity error, the exponential reaching law is selected to be:

$$\dot{s}_i\,(t) = -\gamma s_i\,(t) \tag{5}$$

where $\gamma > 0$, and it is the sliding parameter, it determines the convergence speed of the sliding surface. Taking the time derivative of $s_i(t)$ described in (4), then $\dot{s}_i(t)$ can be obtained as:

$$\begin{aligned} \dot{s}_i\,(t) = \dot{a}_i\,(t) &+ (1+\varepsilon_i)\,k_1 \sum_{j \epsilon \Pi_{i_1}} v_i\,(t) - v_j\,(t) \\ &+ (1-\varepsilon_i)\,k_1 \sum_{j \epsilon \Pi_{i_2}} v_i\,(t) - v_j\,(t) \\ &+ (1+\varepsilon_i)\,k_2 \sum_{j \epsilon \Pi_{i_1}} a_i\,(t) - a_j\,(t) \\ &+ (1-\varepsilon_i) k_2 \sum_{j \epsilon \Pi_{i_2}} a_i(t) - a_j(t) \end{aligned} \tag{6}$$

Therefore $\dot{a}_i\,(t)$ can be rewritten as:

$$\begin{aligned} \dot{a}_i\,(t) = -\gamma s_i\,(t) &- (1+\varepsilon_i)\,k_1 \sum_{j \epsilon \Pi_{i_1}} v_i\,(t) - v_j\,(t) \\ &- (1-\varepsilon_i)\,k_1 \sum_{j \epsilon \Pi_{i_2}} v_i\,(t) - v_j\,(t) \\ &- (1+\varepsilon_i)\,k_2 \sum_{j \epsilon \Pi_{i_1}} a_i\,(t) - a_j\,(t) \end{aligned}$$

$$-(1-\varepsilon_i)k_2\sum_{j\epsilon\Pi_{i_2}} a_i(t)-a_j(t) \tag{7}$$

Combining (3), (4) and (7), the equivalent control input $u_i(t)$ can be obtained:

$$\begin{aligned} u_i(t) = m_i\tau_i[&-\gamma s_i(t)-(1+\varepsilon_i)k_1\sum_{j\epsilon\Pi_{i_1}} v_i(t)-v_j(t)\\ &-(1-\varepsilon_i)k_1\sum_{j\epsilon\Pi_{i_2}} v_i(t)-v_j(t)\\ &-(1+\varepsilon_i)k_2\sum_{j\epsilon\Pi_{i_1}} a_i(t)-a_j(t)\\ &-(1-\varepsilon_i)k_2\sum_{j\epsilon\Pi_{i_2}} a_i(t)-a_j(t)+\hat{\theta}^T\omega]\\ &+m_i a_i(t) \end{aligned} \tag{8}$$

Take $K=[k_1 k_2]$.$\hat{\theta}$ is the estimated value of θ. Considering the fact the vehicle's parameters can be hard to obtain in reality. $\hat{\theta}$ is used for estimation, it refers to the nominal values in Table 1. $\hat{\theta}$ creates parameter mismatches, which adds practical value to this study.

B. STABILITY ANALYSIS

Theorem 1: When the control law in (8) is implemented to the vehicle dynamics in (3), the sliding surface satisfies with the Lyapunov stability, the stability of the platoon can be guaranteed, and the tracking error converges to zero asymptotically.

Proof: The Lyapunov function candidate is selected to be:

$$V_i(t)=\frac{1}{2}s_i(t)^2 \tag{9}$$

The time derivative of the Lyapunov function can be described as:

$$\dot{V}_i(t)=s_i(t)\dot{s}_i(t) \tag{10}$$

Based on (4), (5) and (6), $\dot{V}_i(t)$ can be obtained as:

$$\begin{aligned} \dot{V}_i(t) &= s_i(t)\,\dot{s}_i(t)\\ &= [-\frac{a_i(t)}{\tau_i}+\frac{u_i(t)}{m_i\tau_i}-\hat{\theta}^T\omega\\ &\quad+(1+\varepsilon_i)k_1\sum_{j\epsilon\Pi_{i_1}} v_i(t)-v_j(t)\\ &\quad+(1-\varepsilon_i)k_1\sum_{j\epsilon\Pi_{i_2}} v_i(t)-v_j(t)\\ &\quad+(1+\varepsilon_i)k_2\sum_{j\epsilon\Pi_{i_1}} a_i(t)-a_j(t)\\ &\quad+(1-\varepsilon_i)k_2\sum_{j\epsilon\Pi_{i_2}} a_i(t)-a_j(t)]\\ &\quad\times[a_i(t)+(1+\varepsilon_i)k_1\sum_{j\epsilon\Pi_{i_1}} p_i(t)-p_j(t)-d_{ij}\\ &\quad+(1-\varepsilon_i)k_1\sum_{j\epsilon\Pi_{i_2}} p_i(t)-p_j(t)-d_{ij}\\ &\quad+(1+\varepsilon_i)k_2\sum_{j\epsilon\Pi_{i_1}} v_i(t)-v_j(t)\\ &\quad+(1-\varepsilon_i)k_2\sum_{j\epsilon\Pi_{i_2}} v_i(t)-v_j(t)]\\ &= -\gamma s_i(t)^2 \end{aligned} \tag{11}$$

Since $\gamma>0$, $\dot{V}_i(t)$ is a negative definite. Thus $u_i(t)$ will satisfy the approaching and sliding condition $s_i(t)\dot{s}_i(t)<0$, which guarantees that the trajectory reaches the sliding mode in a finite time and stay there after, therefore the condition for Lyapunov stability is satisfied. The proof of *Theorem 1* is completed.

C. STRINGSTABILITY ANALYSIS

This section implements the Riccati inequality and Lyapunov analysis to solve the controllers' gain, after which the closed-loop error dynamic is analyzed and the system is proved to be string stable.

The closed-loop error is defined as:

$$\begin{aligned} E^T &= [e_1(t)^T\ldots e_N(t)^T],\\ e_i(t) &= \begin{bmatrix}\Delta p_i(t) & \Delta v_i(t)\end{bmatrix}^T.\\ \Delta p_i(t) &= p_i(t)-p_0(t)-d_{i0},\\ \Delta v_i(t) &= v_i(t)-v_0(t) \end{aligned} \tag{12}$$

The closed-loop error dynamic of E^T is:

$$\dot{E}=(I_N\otimes A)E+(I_N\otimes B)Y \tag{13}$$

where

$$Y=\begin{bmatrix}a_1(t)-a_0(t)\\ \cdots\\ a_N(t)-a_0(t)\end{bmatrix},\quad A=\begin{bmatrix}0&1\\0&0\end{bmatrix},\quad B=\begin{bmatrix}0\\1\end{bmatrix}.$$

After the platoon dynamics reach the sliding surface, combining $s_i(t)=0$ into (7), $a_i(t)$ can be rewritten as:

$$\begin{aligned} a_i(t) = &-(1+\varepsilon_i)k_1\sum_{j\epsilon\Pi_{i_1}} p_i(t)-p_j(t)-d_{ij}\\ &-(1-\varepsilon_i)k_1\sum_{j\epsilon\Pi_{i_2}} p_i(t)-p_j(t)-d_{ij}\\ &-(1+\varepsilon_i)k_2\sum_{j\epsilon\Pi_{i_1}} v_i(t)-v_j(t)\\ &-(1-\varepsilon_i)k_2\sum_{j\epsilon\Pi_{i_2}} v_i(t)-v_j(t) \end{aligned} \tag{14}$$

It yields that:

$$Y+(H_\varepsilon\otimes K)E=-1_N a_0(t) \tag{15}$$

where $1_N\in\mathbb{R}^N$, it is the vector with entries that are all one. Substituting (15) into (13), the sliding dynamics of the platoon is:

$$\dot{E}=[I_N\otimes A-H_\varepsilon\otimes(BK)]E-(1_N\otimes B)a_0(t) \tag{16}$$

where $a_0(t)$ is bounded, therefore can be treated as equivalent external disturbance ϖ. A maximum bound for $\varpi^T\varpi$ can be easily found. $\dot{E}$ can be written as:

$$\dot{E} = [I_N \otimes A - H_\varepsilon \otimes (BK)]E - (1_N \otimes B)\varpi \tag{17}$$

Definition 1 [30]: For the m dimensional space of piecewise continuous, square-integrable functions, the norm $\mathcal{L}_2$ is defined by

$$\| x \|_{\mathcal{L}_2} = \sqrt{\int_0^\infty \| x \|^2 dt} < \infty \tag{18}$$

where $\| x \| = \sqrt{x^T x}$, the space is denoted by $\mathcal{L}_2^m$.

Lemma 1 [30]: The platoon system is input-to-output $\mathcal{L}_2$ string stable if all inputs belong to $\mathcal{L}_2$ space, i.e. $\| \varpi \|_{\mathcal{L}_2} < \infty$, and the outputs are once again in the $\mathcal{L}_2$ space for any platoon length $m \in \mathbb{N}$, with the $\mathcal{L}_2$ gain bounded by γ, as shown in below:

$$\| \mathcal{G}_{\varpi E} \|_\infty \triangleq sup \frac{\| E \|_{\mathcal{L}_2}}{\| \varpi \|_{\mathcal{L}_2}} < \gamma \tag{19}$$

Lemma 2 [31]: Given $\in \mathbb{R}^{N\times N}$, then A is Hurwitz if and of if there exists a positive definite matrix $P > 0$, such that:

$$AP + PA^T < 0 \tag{20}$$

Then, Lyapunov function is selected to be:

$$V = E^T \left(Q \otimes \bar{P}\right) E > 0 \tag{21}$$

where $\bar{P} = P^{-1}$. According to the LMI-based method proposed in [31], the following theory can convert the problem into a standard LMI problem:

Theorem 2: Consider the platoon in (3) if there exist matrices $P^T = P > 0 \in \mathbb{R}^{2\times 2}$ and $Q^T = Q > 0 \in \mathbb{R}^{2\times 2}$ such that (22-23) hold.

$$\begin{bmatrix} AP + PA^T + \left(1 - \frac{\lambda_{min}(H_\varepsilon)}{2}\right) BB^T & P \\ P & -\frac{1}{\rho} \end{bmatrix} < 0 \tag{22}$$

$$H_\varepsilon^T Q + QH_\varepsilon - 2\lambda_{min}(H_\varepsilon) Q > 0 \tag{23}$$

where $\lambda_{min}(H_\varepsilon)$ is the minimum eigenvalue of the topological matrix defined in Section II, scalar $\rho > 0$. Then with the feedback gain K as defined as (24), the platoon is input-to-output $\mathcal{L}_2$ string stable for all nonzero $\varpi(t)$.

$$K = \frac{1}{2} B^T P^{-1} \tag{24}$$

The disturbance propagation of the platoon can be described by (25):

$$sup \frac{\| E \|_{\mathcal{L}_2}}{\| \varpi \|_{\mathcal{L}_2}} < \sqrt{\frac{\lambda_{max}(Q)}{\rho\lambda_{min}(Q)}} \tag{25}$$

Proof: Taking the time derivative of V

$$\begin{aligned} \dot{V} &= \dot{E}^T \left(Q \otimes \bar{P}\right) E + E^T \left(Q \otimes \bar{P}\right) \dot{E} \\ &= E^T [Q \otimes (A^T \bar{P}) - ({H_\varepsilon}^T Q) \otimes (BK)^T \bar{P} + Q \otimes (\bar{P}A) \\ &\quad - (QH_\varepsilon) \otimes (\bar{P}BK)]E + \varpi^T [Q \otimes (B^T \bar{P})]E \\ &\quad + E^T [Q \otimes \left(\bar{P}B\right)]\varpi \end{aligned} \tag{26}$$

Substitutes (24) into (26), $\dot{V}$ be rewritten as:

$$\begin{aligned} \dot{V} &= -E^T [({H_\varepsilon}^T Q) \otimes (\frac{1}{2}\bar{P}BB^T\bar{P}) + (QH_\varepsilon) \otimes (\frac{1}{2}\bar{P}BB^T\bar{P})]E \\ &\quad + E^T [Q \otimes (A^T \bar{P}) + Q \otimes (\bar{P}A)]E + \varpi^T [Q \otimes (B^T \bar{P})]E \\ &\quad + E^T [Q \otimes (\bar{P}B)]\varpi \end{aligned} \tag{27}$$

It can be obtained that:

$$\begin{aligned} &\varpi^T [Q \otimes (B^T \bar{P})]E + E^T [Q \otimes (\bar{P}B)]\varpi \\ &\quad \le E^T \left[Q \otimes \left(\bar{P}BB^T\bar{P}\right)\right] E \\ &\quad + \lambda_{max}(Q)\, \varpi^T \varpi \end{aligned} \tag{28}$$

To prove (28) holds, it can be transformed into:

$$\begin{bmatrix} E \\ \varpi \end{bmatrix}^T \begin{bmatrix} Q \otimes (\bar{P}BB^T\bar{P}) & -Q \otimes (\bar{P}B) \\ -Q \otimes (B^T\bar{P}) & \lambda_{max}(Q) \end{bmatrix} \begin{bmatrix} E \\ \varpi \end{bmatrix} \ge 0 \tag{29}$$

Using Schur complement, (29) is equivalent to:

$$(Q^{-1} - \frac{1}{\lambda_{max}(Q)} I_N) \otimes (\bar{P}BB^T\bar{P}) \ge 0 \tag{30}$$

Given that $\lambda\left(Q^{-1}\right) = \frac{1}{\lambda(Q)}$, (30) holds, therefore, (28) holds. substituting (28) into (27), $\dot{V}$ is rewritten as:

$$\begin{aligned} \dot{V} &= -E^T [({H_\varepsilon}^T Q) \otimes (\frac{1}{2}\bar{P}BB^T\bar{P}) + (QH_\varepsilon) \otimes (\frac{1}{2}\bar{P}BB^T\bar{P})]E \\ &\quad + E^T [Q \otimes (A^T\bar{P}) + Q \otimes (\bar{P}A)]E \\ &\quad + E^T \left[Q \otimes (\bar{P}BB^T\bar{P})\right] E \\ &\quad + \lambda_{max}(Q)\, \varpi^T \varpi \end{aligned} \tag{31}$$

For the first two terms in (31), given inequality (23), the following inequality holds:

$$\begin{aligned} &E^T [-(H_\varepsilon^T Q) \otimes (\frac{1}{2}\bar{P}BB^T\bar{P}) - (QH_\varepsilon) \otimes (\frac{1}{2}\bar{P}BB^T\bar{P}) \\ &\quad + Q \otimes (A^T\bar{P}) + Q \otimes (\bar{P}A)]E \\ &< -E^T \left[\left(QH_\varepsilon + H_\varepsilon^T Q - Q\right) \otimes \left(\frac{\lambda_{min}(H_\varepsilon)}{2} \bar{P}BB^T\bar{P}\right)\right] E \\ &\quad + E^T [Q \otimes (A^T\bar{P} + \bar{P}A - \frac{\lambda_{min}(H_\varepsilon)}{2} \bar{P}BB^T\bar{P})]E \\ &< E^T [Q \otimes (A^T\bar{P} + \bar{P}A - \frac{\lambda_{min}(H_\varepsilon)}{2} \bar{P}BB^T\bar{P})]E \end{aligned} \tag{32}$$

Then we have:

$$\begin{aligned} &\rho\lambda_{min}(Q) \left[E^T E - \frac{\lambda_{max}(Q)}{\rho\lambda_{min}(Q)} \varpi^T\varpi\right] + \dot{V} \\ &\quad \le \rho E^T (Q \otimes I) E \\ &\quad - \lambda_{max}(Q)\, \varpi^T\varpi + \dot{V} \end{aligned} \tag{33}$$

Substitute (31) and (32) into (33), it can be obtained that:

$$\begin{aligned} &\rho\lambda_{min}(Q) \left[E^T E - \frac{\lambda_{max}(Q)}{\rho\lambda_{min}(Q)} \varpi^T\varpi\right] + \dot{V} \\ &\quad \le E^T [Q \otimes (A^T\bar{P} + \rho I \end{aligned}$$

$$+\bar{P}A-(1-\frac{\lambda_{min}(H_\varepsilon)}{2})\bar{P}BB^T\bar{P})]E \quad (34)$$

Given LMI (22), (34) can be transformed into:

$$\rho\lambda_{min}(Q)\left[E^TE-\frac{\lambda_{max}(Q)}{\rho\lambda_{min}(Q)}\varpi^T\varpi\right]+\dot{V}<0 \quad (35)$$

(35) is equivalent to:

$$\int_{t=0}^{+\infty}[E^TE-\frac{\lambda_{max}(Q)}{\rho\lambda_{min}(Q)}\varpi^T\varpi]dt < \frac{1}{\rho\lambda_{min}(Q)}[V|_0^{+\infty}-\int_0^{+\infty}\dot{V}dt] \quad (36)$$

From (36), it can be derived that:

$$\int_{t=0}^{+\infty}\parallel E\parallel_{\mathcal{L}_2}^2dt-\frac{\lambda_{max}(Q)}{\rho\lambda_{min}(Q)}\int_{t=0}^{+\infty}\parallel\varpi\parallel_{\mathcal{L}_2}^2dt<0 \quad (37)$$

It can be observed that:

$$\parallel E\parallel_{\mathcal{L}_2}^2<\frac{\lambda_{max}(Q)}{\rho\lambda_{min}(Q)}\parallel\varpi\parallel_{\mathcal{L}_2}^2 \quad (38)$$

Given that $a_0(t)$ is bounded and treated as equivalent external disturbance ϖ, thus a maximum bound for $\varpi^T\varpi$ can be easily found, which is equivalent to $\max(a_0(t)^2)$. The specific value of $a_0(t)$ is defined in the Section V. $\max\left(\varpi^T\varpi\right)=4$. Therefore, it can be obtained that:

$$\parallel\varpi(t)\parallel_{\mathcal{L}_2}<\infty \quad (39)$$

Therefore, the condition for input-to-output $\mathcal{L}_2$ string is satisfied, where $\gamma=\sqrt{\frac{\lambda_{max}(Q)}{\rho\lambda_{min}(Q)}}$. The proof of *Theorem 2* is completed.

IV. MULT-OBJECTIVE HETEROGENEOUS ASYMMETRIC DEGREES OPTIMISATION

A. PLATOON PERFORMANCE EVALUATION

Three performance indices are used as the platoon performance assessment criteria in order to examine the effect of different topologies on CAV platoon performance. They were discussed in our previous work [8], [10]. The first one is the tracking index (TI) [29], which shows a vehicle's ability to track a preceding vehicle. TI for the ith vehicle is expressed as:

$$TI_i=\frac{1}{T}\int_0^T(|\Delta v_i(t)\,SVE|+|\Delta p_i(t)SDE|)dt \quad (40)$$

where T is the total simulation length, $\Delta v_i(t)$ and $\Delta p_i(t)$ are defined in (12). $SVE=20$ represents the velocity error sensitivity and $SDE=50$ represents the spacing error sensitivity [29].

The second index is fuel consumption [32] that indicates how much fuel the vehicle consumes. The fuel consumption for the ith vehicle is expressed as

$$F_i(t)=\begin{cases}\xi_0+\xi_1P_i(t)+\xi_2P_i(t)^2, & P_i(t)\geq 0\\ \xi_0, & P_i(t)<0\end{cases} \quad (41)$$

$$P_i(t)=(\frac{R_i(t)+1.04m_ia_i(t)}{3600\eta})v_i(t) \quad (42)$$

TABLE 1. Vehicle dynamics parameters for the platoon.

Symbol	Description	Units	Range	Nominal
m	Vehicle mass	kg	1200-1700	1500
K_d	Aerodynamic resistance coefficient	-	0.2536	0.2536
v_a	Wind speed	m/s	-5-5	-5-5
g	Gravitational acceleration	m/s^2	9.8	9.8
f	Rolling resistance coefficient	-	0.015-0.025	0.010
θ	Grade of the road	$^\circ$	0-3	0-3
η	Driveline efficiency	-	0.8	0.8
C_h	Correction factor	-	1	1
A_f	Vehicle frontal area	m^2	2.08-2.45	2.20
C_r	Road surface coefficient	-	1.75	1.75
ξ_0	Fuel economy index1	-	6×10^{-4}	6×10^{-4}
ξ_1	Fuel economy index2	-	1.9×10^{-5}	1.9×10^{-5}
ξ_2	Fuel economy index3	-	1×10^{-6}	1×10^{-6}
τ	Vehicle engine time	s	0.2-0.6	0.3
d_m	Mechanical drag	N	0-110	50

$$R_i(t)=\frac{\rho}{25.92}K_{di}C_hA_fv_i(t)^2+gm_if\frac{C_r}{1000}+gm_isin\theta \quad (43)$$

where $F_i(t)(L/s)$ is the fuel consumption rate of vehicle i, $P_i(t)$(kw) is the instantaneous power of vehicle i, $R_i(t)$(N) is the total resistance of vehicle i. ξ_0,ξ_1,ξ_2 are unitless parameters, η is the driveline efficiency of vehicle i. C_h is the correction factor. A_f is the vehicle frontal area of vehicle i. C_r is the road surface coefficient. g is the gravitational acceleration, which is $9.8m/s^2$. θ is the grade of the road. f is the rolling resistance coefficent. Because this study considers a platoon of heterogeneous vehicles, all of the above-mentioned parameters are different for each vehicle and are chosen at random within a reasonable range, they are shown in Table 1.

The third index is the acceleration standard deviation (ASD) [29] that indicates the degree of the smooth of the vehicle's velocity profile. ASD for the ith vehicle is expressed as:

$$ASD_i=std(a_i(t)) \quad (44)$$

where std represents the standard deviation in $t\in[0,T]$.

B. NSGA-II BASED HETEROGENEOUS ASYMMETRIC DEGREES OPTIMISATION

Numerous studies have recognized the importance of using an asymmetric degree in the topological matrix [15]–[17]. It is shown that with the asymmetric degree, a constant stability margin that is bounded away from zero is easily obtained regardless of platoon size [15]. It is critical when dealing with platoon with a large size. The Laplacian eigenvalues were

proved to be bounded by a nonzero constant, which provides an excellent way to ensure the platoon's stability, especially in bidirectional topology [16]. Previous research, on the other hand, selected the asymmetric degree arbitrarily without regard for optimisation goals. Moreover, conventional approaches are incapable of determining the optimal heterogeneous asymmetric degrees. Bases on our previous work [8], [10], we suggest a learning algorithm-based solution (NSGA-II algorithm) to this problem. Given that developing mathematical models for heterogeneous asymmetric degrees and platoon performance is neither feasible nor practical, NSGA-II algorithm is a good fit for this problem because it can detect patterns in data without the use of mathematical models. Furthermore, in terms of searching for heterogeneous asymmetric degrees for each vehicle, this control problem has a large number of independent input variables. When the platoon size increases, so does the number of inputs. Traditional methods are incapable of dealing with large numbers of input variables, however, NSGA-II algorithm excels in this area. Overall, NSGA-II algorithm is a good fit for the control problem.

The key point of applying the NSGA-II algorithm to the process is to find optimal heterogeneous asymmetric degrees, which are then added to the topological matrix. Thus, a new matrix's minimum eigenvalue can be obtained. The gain of the controller can be solved using the LMI approach based on the eigenvalue. Thus, the latest control input can be obtained, as well as the corresponding platoon performance indices. The following summarizes the NSGA-II algorithm for computing the optimal heterogeneous asymmetric degrees.

NSGA-II algorithm

Data: input: heterogeneous asymmetric degrees ε_i. N: size of the initial population; n: number of iterations, f_1 (x): Tracking index; f_2 (x): Fuel consumption; f_3 (x): Acceleration standard deviation.
Initialise population:
Generate random population for ε_i
Generate new topological matrix and calculate new minimum eigenvalue
Solve LMI (22-23)
Calculate the controllers' gain using (24)
Calculate the control input using (8)
Calculate the objective values: f_1 (x) , f_2 (x) , f_3 (x)
Sort the initial population with size N
Calculate the rank using f_1 (x) , f_2 (x) , f_3 (x) as objectives
Assign crowding distance to the initial population
For i=1: n
Perform selection
Create a mating pool
Perform genetic operator (Crossover and Mutation)
Combine the population
Perform selection
end

V. SIMULATION AND RESULTS

The simulation is conducted on MATLAB, written in C programming language. The platoon is modelled using Simulink. The simulation was conducted on an Intel Core i7-8550U laptop, with 1.8GHz and a RAM of 8GB. Numerical simulations are conducted to illustrate the main results. A platoon with eleven heterogeneous vehicles (one leader and ten followers) interconnected by asymmetric topologies are considered. Two scenarios and four information flow topologies are considered in the simulations. To show the superiority of the proposed method, symmetric control is tested first, homogeneous asymmetric control is tested secondly. Finally, the proposed heterogeneous asymmetric sliding mode control method is tested.

TABLE 2. The Initial States And Desired Gaps Of Each Vehicle Under Urban Road Scenario.

Vehicle Index	Position (m)	Velocity (m/s)	Desired Gap (m)
Vehicle1	-20	3	-20
Vehicle2	-49	5	-40
Vehicle3	-61	3.5	-60
Vehicle4	-78	4.2	-80
Vehicle5	-102	3.8	-100
Vehicle6	-123	4.4	-120
Vehicle7	-137	4.1	-140
Vehicle8	-161	3.7	-160
Vehicle9	-182	4.2	-180
Vehicle10	-202	4.1	-200

A. SCENARIO DESIGN

1) URBAN ROAD CASE STUDY

This study considers two traffic scenarios. The first one is the urban road scenario, as most people drive on urban roads on a daily basis. According to the general speed limit on urban roads in Australia, a vehicle's top speed should be no more than 14 m/s. The desired gap between two consecutive vehicles should be $20m$. A sine wave is added to the leader's acceleration profile to emphasise the environmental disturbance. The kinematic model for the leader vehicle on urban road is described as:

$$a_0(t) = \begin{cases} 0 & 0 < t \leq 20s \\ 0.5 + 0.5\sin\left(\frac{\pi}{10}t\right) m/s & 20 < t \leq 30s \\ 0 & 30 < t \leq 50s \\ -0.5 + 0.5\sin \otimes (\frac{\pi}{10}t) m/s & 50 < t \leq 60s \\ 0 & 60 < t \leq 100s \end{cases} \quad (45)$$

Each vehicle's initial position, velocity, and the desired distance between itself and the leader vehicle are presented in Table 2.

2) HIGHWAY CASE STUDY

This study considers the highway scenario secondly, as platooning control is essential to releasing traffic congestion, especially on the highway. Referring to Australia's speed limit on the highway, a vehicle's top speed should be no more than $28m/s$. The desired gap between two consecutive vehicles should be $50m$ to ensure safety. The leader vehicle

TABLE 3. The initial states and desired gaps of each vehicle under highway scenario.

Vehicle Index	Position (m)	Velocity (m/s)	Desired Gap (m)
Vehicle1	-51	11	-50
Vehicle2	-99	9	-100
Vehicle3	-152	9.5	-150
Vehicle4	-205	8.8	-200
Vehicle5	-251	10.6	-250
Vehicle6	-297	11.5	-300
Vehicle7	-345	11.3	-350
Vehicle8	-402	10.8	-400
Vehicle9	-449	9.3	-450
Vehicle10	-501	10.2	-550

also experiences an amplified environmental disturbance due to the high speed. The kinematic model for the leader vehicle on highway is described as:

$$a_0(t) = \begin{cases} 0 & 0 < t \leq 20s \\ 1 + \sin\left(\frac{\pi}{10}t\right) m/s & 20 < t \leq 30s \\ 0 & 30 < t \leq 50s \\ -1 + \sin \otimes (\frac{\pi}{10}t) m/s & 50 < t \leq 60s \\ 0 & 60 < t \leq 100s \end{cases} \quad (46)$$

Each vehicle's initial position, velocity, and the desired distance between itself and the leader vehicle are presented in Table 3.

3) CHOICE OF ASYMMETRIC TOPOLOGIES

To investigate the impact of wireless communication and validate the effectiveness of the proposed strategy fully, This study considers three traditional topologies and one random topology in each case study based on its bidirectional complexity. The three traditional topologies are two predecessors single following topology (TPSF), Predecessor-leader following topology (PLF) and Bidirectional-leader topology (BDL). One random topology is also included in this study to prove the effectiveness of the proposed method. Random topology can be common in reality due to unstable wireless communication. To take the packet loss into consideration. This study uses Bernoulli distribution to express the packet drop rate, the packet losses probability increases when the distance between two vehicles increases. Therefore, a fixed predefined random topology can be obtained. They are shown in the Fig.2. below.

One random topology is also included in this study to prove the effectiveness of the proposed method. Random topology can be common in reality due to unstable wireless communication. To take the packet loss into consideration. This study uses Bernoulli distribution to express the packet drop rate, the packet losses probability increases when the distance between two vehicles increases. Therefore, a random topology can be obtained.

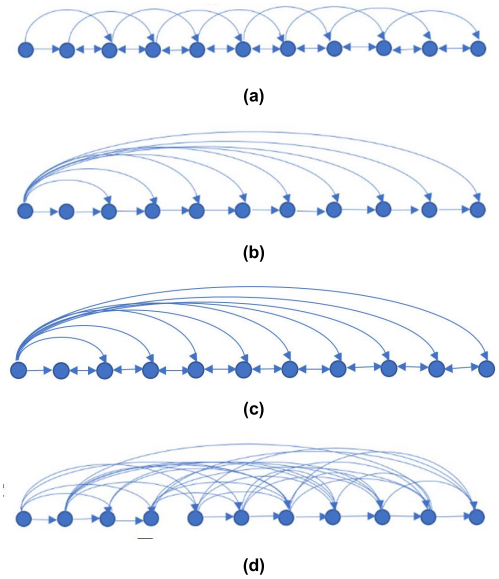

FIGURE 2. Information flow topologies for platoon. (a)TPSF; (b)PLF; (c) BDL; (d) Random.

B. COMPARISONS OF SPACING ERROR

Taking PLF topology for an example, Fig.3 shows the platoon's spacing error in the Highway Case Study. Symmetric control is used firstly, where asymmetric degree is equal to zero, whereas Fig.4 depicts the platoon's spacing error using heterogeneous asymmetric control, which is the strategy proposed in the paper. The figures illustrate that spacing errors are significantly reduced, demonstrating the effectiveness of the proposed method. On highways, all platoons performed worse than on urban roads. It can be concluded that as the desired velocity and gap between vehicles increase, the control problem becomes more difficult.

The most dramatic changes in both case studies occurred in TPSF topology scenario. Spacing errors varied between $6m$ and $11m$ with symmetric control but were reduced to within $0.1m$ with both homogeneous and heterogeneous asymmetric control strategies. Furthermore, the PLF and BDL topologies outperform the others. The proposed strategy reduces the spacing errors from around $2m$ to near zero.

The differences in spacing error between homogeneous asymmetric control and heterogeneous asymmetric control are relatively small, which is difficult to see from the figures solely. However, the proposed strategy is shown to reduce all spacing errors to less than $0.1m$, which is a reasonable threshold for ensuring consensus and stability. After 60 seconds, all platoons reach consensus. It can be concluded that the proposed strategy can significantly reduce platoon's spacing error.

C. COMPARISONS OF VELOCITY ERROR

Fig.5 depicts the platoon's velocity error for BDL topology under the Urban Road Case Study with symmetric control.

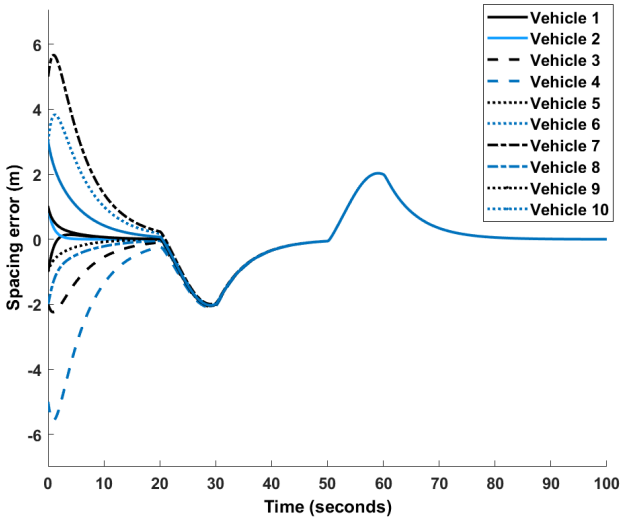

FIGURE 3. Spacing error with symmetric control under highway case study with plf topology.

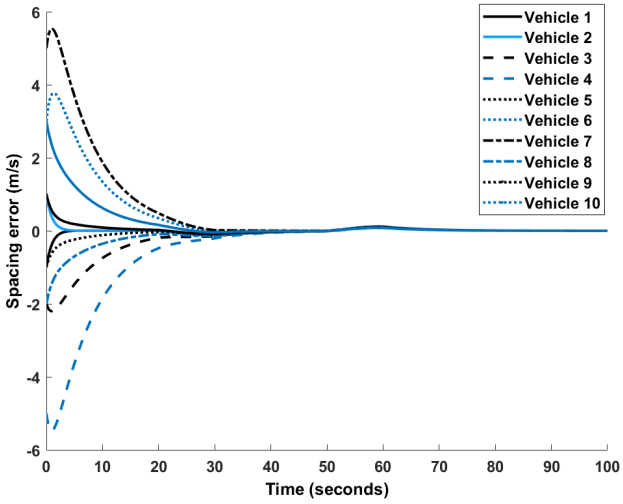

FIGURE 4. Spacing error with asymmetric control under highway case study with PLF topology.

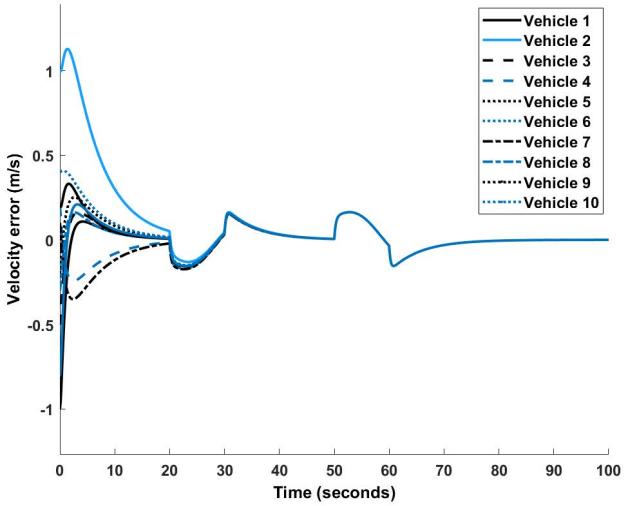

FIGURE 5. Velocity error with symmetric control under urban road case study with BDL topology.

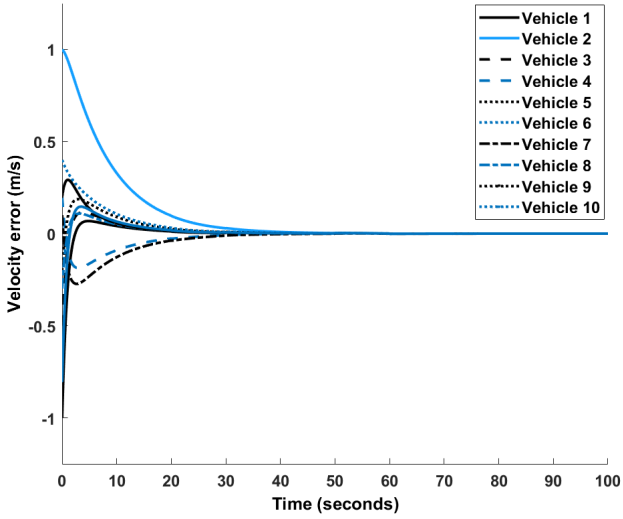

FIGURE 6. Velocity error with asymmetric control under urban road case study with BDL topology.

The resulting velocity errors of heterogeneous asymmetric control is shown in Fig.6. Figures resulting from the Highway Case Study are similar. Velocity errors are greatly reduced in all cases, demonstrating the efficacy of the proposed strategy. All platoons performed better on urban roads than on highways, implying that platoons' velocity consensus is more susceptible to high velocity profiles. The proposed strategy has the greatest impact in both case studies on the TPSF and Random topology, where velocity errors were reduced to within $0.1m/s$ from $2m/s$ and $1m/s$, respectively. Moreover, BDL and PLF topology outperformed the others.

The velocity error differences between homogeneous asymmetric control and heterogeneous asymmetric control are comparatively small. The proposed strategy, on the other hand, is shown to reduce all spacing errors to less than $0.1m/s$. At 50 seconds, all platoons experienced a visible jerk in velocity errors, then achieved consensus at 60 seconds, showing that the proposed method is capable of ensuring platoon velocity consensus.

D. EFFECT ANALYSIS OF CONTROL STRATEGY

Table 4 and Table 5 display the obtained heterogeneous Pareto asymmetric degree in two cases studies.

For the homogeneous asymmetric control method, the Pareto optimal asymmetric degree varies between 59% and 62% for the TPSF, PLF, and BDL topology. The Pareto optimal asymmetric degree for the Random topology is about 82%. In both cases, all vehicles in the platoon have a different optimal asymmetric degree, there is also no regularity observed from the average Pareto optimal asymmetric degree.

On the other hand. Controller's gains are significantly increased in all cases. With the heterogeneous asymmetric controller, the controller's gains have an average increase of 95.71% in the Urban Road Case Study and 96.16% in the

TABLE 4. Heterogeneous optimal asymmetric degree for different information flow topologies under urban road scenario (%).

Vehicle Index	TPSF Topology	PLF Topology	BDL Topology	Random Topology
Vehicle 1	37.7028	4.3866	20.3393	34.4162
Vehicle 2	3.8169	12.3510	79.2367	74.5473
Vehicle 3	24.9679	61.3486	91.7491	55.2489
Vehicle 4	1.9372	36.0972	10.1663	50.1402
Vehicle 5	82.4120	30.6044	28.0382	91.4980
Vehicle 6	36.9815	73.8370	80.5722	26.4492
Vehicle 7	9.4117	30.6501	46.4649	71.1928
Vehicle 8	13.8632	57.7408	48.6109	75.8740
Vehicle 9	25.0637	44.0656	2.6883	37.4992
Vehicle 10	20.3665	28.3544	54.819	53.1265
Average	25.6523	37.9436	46.2831	56.9993

TABLE 5. Heterogeneous optimal asymmetric degree for different information flow topologies under highway scenario (%).

Vehicle Index	TPSF Topology	PLF Topology	BDL Topology	Random Topology
Vehicle 1	28.4906	4.4420	81.0039	55.2742
Vehicle 2	57.4713	13.7518	6.0768	58.6238
Vehicle 3	18.2702	46.2187	7.4281	68.8742
Vehicle 4	61.7325	86.5203	24.7905	28.6852
Vehicle 5	65.5942	30.3635	40.6708	89.7491
Vehicle 6	44.0005	26.2930	63.4554	74.4241
Vehicle 7	11.6403	7.5736	24.5636	10.9627
Vehicle 8	39.8982	5.0993	65.3486	25.7540
Vehicle 9	56.2715	54.3244	52.2687	85.9057
Vehicle 10	30.3013	78.5097	4.1552	10.3265
Average	41.3670	35.3096	36.9761	50.8580

Highway Case Study. Increased controller gains can significantly improve platoon performance. However, this does not imply that the higher the controller's gains, the better the platoon's performance, as will be discussed in greater detail in the following subsections.

Fig. 7 shows the obtained Pareto fronts in the Urban Road Case Study using the proposed strategy with TPSF and Random topology. Figures resulting from the Highway Case Study are similar. Because the Pareto front varies depending on the road and topology scenario, the resemblance between graphs is negligible, implying that no linear correlations exist between the heterogeneous asymmetric degrees and the platoon's three primary performance indices. Furthermore, despite the fact that the optimal heterogeneous asymmetric degrees cannot be calculated using a traditional mathematical formula, NSGA-II learning algorithm is well suited to this control problem.

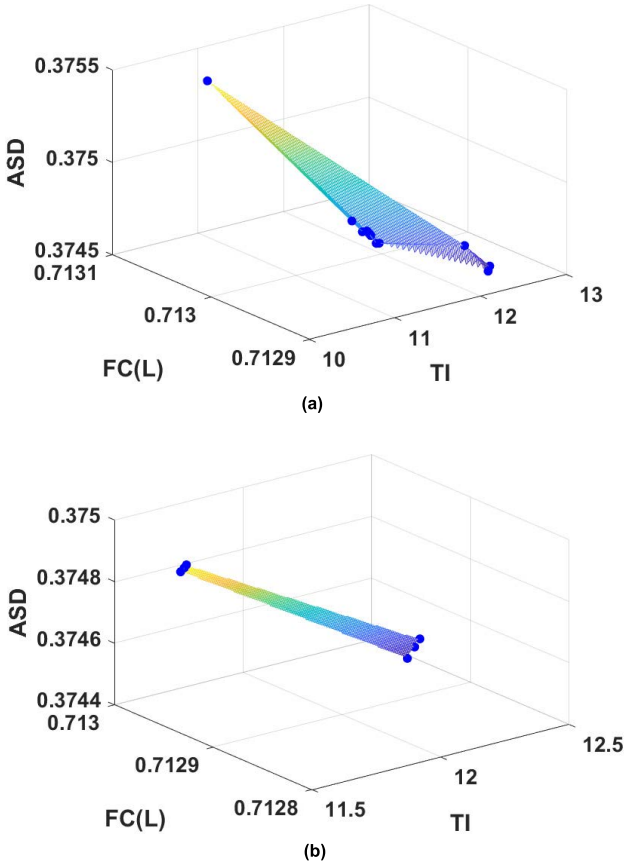

FIGURE 7. Pareto front with heterogeneous asymmetric control under Urban Road Case Study. (a) TPSF; (b)Random.

The three performance assessment criteria addressed in this study are the tracking index, fuel consumption, and acceleration standard deviation. They are used to undertake a thorough and comprehensive assessment of a platoon's performance.

1) TRACKING ABILITY

The tracking index demonstrates a vehicle's ability to track the vehicles in front of it in the platoon. Since it is calculated using spacing and velocity errors, the lower the tracking index, the better the tracking ability.

Table 6 shows the tracking index for four different topologies in the Urban Road Case Study, using vehicle 1, 5, 10, and the platoon as examples.

For homogeneous and heterogeneous asymmetric control, the platoon's tracking index improved by an average of 55.09% and 60.68%, respectively. The proposed scheme has the largest impact on the TPSF topology, raising its tracking index by 77.68% while only increasing the PLF topology's tracking index by 46.97%. Table 7 also displays the tracking index for the Highway Case Study. For homogeneous and heterogeneous asymmetric control, the platoon's tracking index improved by an average of 73.84% and 76.2%, respectively. In contrast to the Urban Road Case Study, the proposed approach improved the tracking ability of the TPSF

TABLE 6. Tracking index for different information flow topologies under urban road scenario.

Information Flow Topology	Control Strategy	Vehicle 1	Vehicle 5	Vehicle 10	Platoon Overall
TPSF	Symmetric	1.81	4.427	6.6901	47.71
	Homogeneous	0.4512	1.068	0.856	12.29
	Heterogeneous	**0.3872**	**0.9335**	**0.7566**	**10.65**
PLF	Symmetric	1.68	2.068	1.92	21.97
	Homogeneous	0.4986	1.155	0.9205	13.47
	Heterogeneous	**0.4827**	**1.014**	**0.8127**	**11.65**
BDL	Symmetric	1.734	2.116	1.869	22.59
	Homogeneous	0.5007	1.157	0.8956	13.4
	Heterogeneous	**0.4555**	**1.056**	**0.7543**	**12.02**
Random	Symmetric	3.211	4.136	4.158	40.4
	Homogeneous	0.4985	1.157	0.925	13.44
	Heterogeneous	**0.4549**	**1.017**	**0.8229**	**11.61**

TABLE 7. Tracking index for different information flow topologies under highway scenario.

Information Flow Topology	Control Strategy	Vehicle 1	Vehicle 5	Vehicle 10	Platoon Overall
TPSF	Symmetric	3.065	7.632	13.28	87.4
	Homogeneous	0.1052	0.3094	1.032	11.7
	Heterogeneous	**0.1026**	**0.2839**	**0.9497**	**10.77**
PLF	Symmetric	2.673	2.753	3.314	34.11
	Homogeneous	0.0970	0.278	1.17	12.65
	Heterogeneous	**0.2365**	**0.3411**	**1.026**	**11.44**
BDL	Symmetric	2.638	2.730	3.116	34.23
	Homogeneous	0.102	0.2827	1.089	12.56
	Heterogeneous	**0.0939**	**0.2635**	**0.9765**	**11.47**
Random	Symmetric	5.863	6.949	7.871	71.8
	Homogeneous	0.1009	0.29	1.166	12.54
	Heterogeneous	**0.1868**	**0.3618**	**1.064**	**11.36**

and PLF topologies by 87.68% and 66.46%, respectively. Fig.8 compares platoon's tracking index across four different topologies in both case studies to provide an intuitive view.

It is can be concluded that the proposed heterogeneous asymmetric control strategy outperforms the homogeneous asymmetric control strategy. When dealing with platoons travelling at a reasonably high velocity and requiring wide inter-vehicle gaps, the proposed approach is more successful.

2) FUEL ECONOMY

Fuel economy is another important platoon's property that is measured in terms of fuel consumption. The vehicle's fuel efficiency increases as the amount of fuel used decreases. Tables 8 and 9 demonstrate the fuel consumption for various

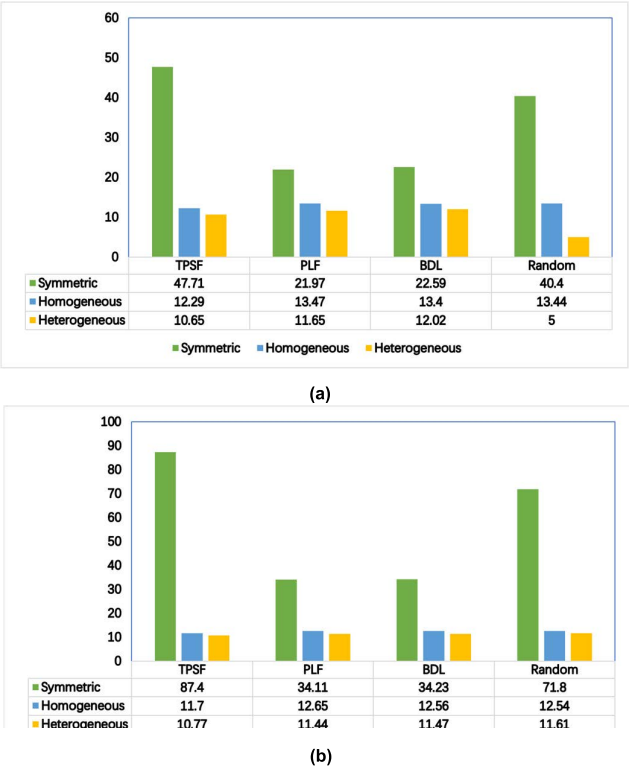

FIGURE 8. Tacking index comparison. (a) Urban road; (b) Highway.

TABLE 8. Fuel consumption for different information flow topologies under urban road scenario (L).

Information Flow Topology	Control Strategy	Vehicle 1	Vehicle 5	Vehicle 10	Platoon Overall
TPSF	Symmetric	0.0643	0.0664	0.0661	0.7193
	Homogeneous	0.0642	0.0657	0.0649	0.7129
	Heterogeneous	**0.0642**	**0.0657**	**0.0650**	**0.7131**
PLF	Symmetric	0.0643	0.0659	0.0651	0.7142
	Homogeneous	0.0642	0.0657	0.0649	0.7129
	Heterogeneous	**0.0642**	**0.0657**	**0.0649**	**0.7130**
BDL	Symmetric	0.0643	0.0659	0.0651	0.7142
	Homogeneous	0.0642	0.0657	0.0649	0.7129
	Heterogeneous	**0.0642**	**0.0657**	**0.0649**	**0.7129**
Random	Symmetric	0.0644	0.0663	0.0654	0.7172
	Homogeneous	0.0642	0.0657	0.0649	0.7129
	Heterogeneous	**0.0642**	**0.0657**	**0.0649**	**0.7130**

topologies in the Urban Road and Highway Case Study. The tables show that the proposed approach reduces the fuel consumption of all vehicles, and the platoon consumed more fuel on the highway than on the urban road in general. Changes in fuel consumption, on the other hand, are less vulnerable to changes in control strategy. Fuel economy is still improved by an average of 0.4633% and 0.4494% with the homogeneous and heterogeneous asymmetric control, respectively, in the

TABLE 9. Fuel consumption for different information flow topologies under highway scenario (L).

Information Flow Topology	Control Strategy	Vehicle 1	Vehicle 5	Vehicle 10	Platoon Overall
TPSF	Symmetric	0.1089	0.1394	0.1342	1.383
	Homogeneous	0.1068	0.1296	0.1179	1.293
	Heterogeneous	**0.1068**	**0.1296**	**0.1179**	**1.293**
PLF	Symmetric	0.1083	0.1320	0.1198	1.313
	Homogeneous	0.1068	0.1295	0.1178	1.293
	Heterogeneous	**0.1069**	**0.1269**	**0.1179**	**1.293**
BDL	Symmetric	0.1083	0.1320	0.1197	1.313
	Homogeneous	0.1068	0.1295	0.1178	1.293
	Heterogeneous	**0.1068**	**0.1295**	**0.1178**	**1.293**
Random	Symmetric	0.1108	0.1378	0.1247	1.355
	Homogeneous	0.1068	0.1295	0.1178	1.293
	Heterogeneous	**0.1069**	**0.1296**	**0.1179**	**1.293**

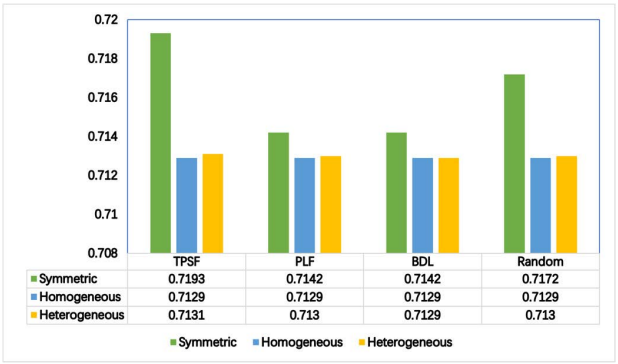

(a)

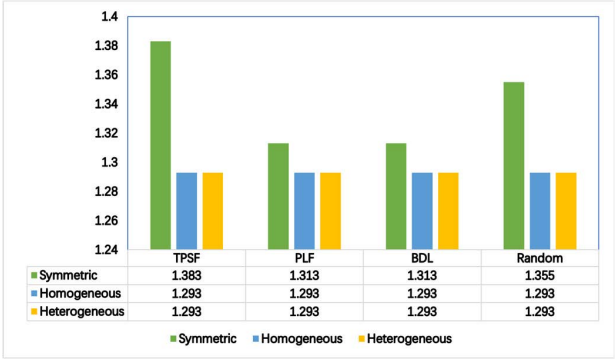

(b)

FIGURE 9. Fuel consumption (L) comparison. (a) Urban Road; (b) Highway.

Urban Road Case Study. Fuel economy is improved by an average of 3.5324% for all asymmetric control methods in the Highway Case Study. In both case studies, Fig.9 compares platoon fuel consumption over four different topologies to provide a clear overview.

Both asymmetric control methods clearly boost platoon fuel economy to nearly the same extent, particularly

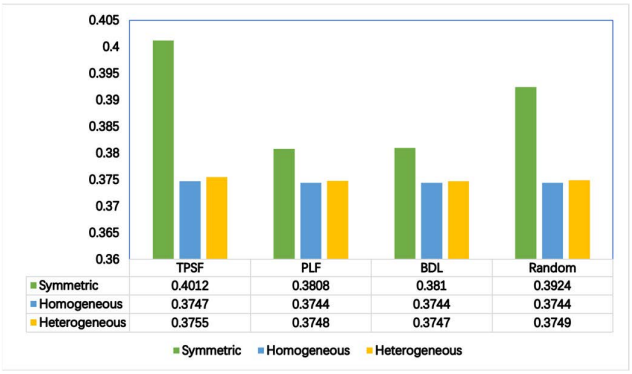

(a)

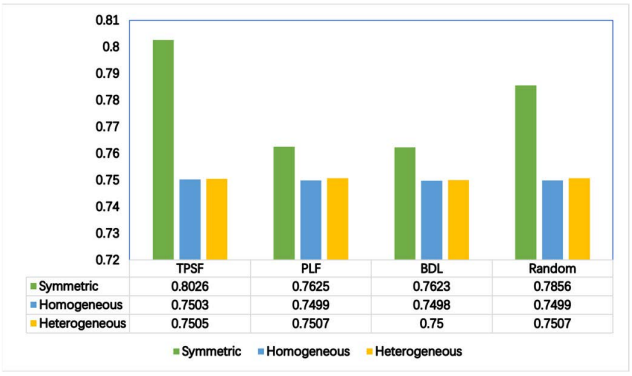

(b)

FIGURE 10. Acceleration standard deviation comparison. (a) Urban road; (b) Highway.

on highways. Furthermore, the proposed approach has the greatest impact on the TPSF topology's fuel efficiency, improving it by 0.8619% and 6.5076% under the Urban Road and Highway Case Studies, respectively.

3) DRIVING COMFORT

Because it reflects the smoothness of the profile, the acceleration standard deviation (ASD) is used to measure the platoon's driving comfort. Smooth and comfortable driving has long been recognised as an essential role of the intelligent vehicle system. The smaller the ASD, the better the driving experience. Tables 10 and 11 show the ASD for four different topologies in the Urban Road and Highway Case Study. The tables show that the suggested approach reduces the ASD of all vehicles, and the platoon has more driving comfort on the urban road than on the highway in general. Driving comfort is increased by an average of 3.6513% and 3.5237% with the homogeneous and heterogeneous asymmetric control, respectively, in the Urban Road Case Study. In the Highway Case Study, homogeneous and heterogeneous asymmetric control increase driving comfort by an average of 3.5882% and 3.5237%, respectively. Fig.10 shows platoon's acceleration standard deviation over four different topologies in both case studies to present a good overview.

Both asymmetric control methods clearly enhance platoon's driving comfort to nearly the same amount,

TABLE 10. Acceleration standard deviation for different information flow topologies under urban road scenario.

Information Flow Topology	Control Strategy	Vehicle 1	Vehicle 5	Vehicle 10	Platoon Overall
TPSF	Symmetric	0.3879	0.3967	0.4236	0.4012
	Homogeneous	0.3803	0.3735	0.3791	0.3747
	Heterogeneous	**0.3808**	**0.3742**	**0.3810**	**0.3755**
PLF	Symmetric	0.3854	0.3798	0.3849	0.3808
	Homogeneous	0.3801	0.3732	0.3784	0.3744
	Heterogeneous	**0.3806**	**0.3737**	**0.3791**	**0.3748**
BDL	Symmetric	0.3860	0.3800	0.3856	0.3810
	Homogeneous	0.3801	0.3732	0.3786	0.3744
	Heterogeneous	**0.3803**	**0.3734**	**0.3796**	**0.3747**
Random	Symmetric	0.3943	0.3924	0.3981	0.3924
	Homogeneous	0.3801	0.3732	0.3784	0.3744
	Heterogeneous	**0.3806**	**0.3738**	**0.3791**	**0.3749**

TABLE 11. Acceleration standard deviation for different information flow topologies under highway scenario.

Information Flow Topology	Control Strategy	Vehicle 1	Vehicle 5	Vehicle 10	Platoon Overall
TPSF	Symmetric	0.7641	0.7920	0.8365	0.8026
	Homogeneous	0.7481	0.7460	0.7469	0.7503
	Heterogeneous	**0.7481**	**0.7460**	**0.7467**	**0.7505**
PLF	Symmetric	0.7595	0.7580	0.7581	0.7625
	Homogeneous	0.7481	0.7458	0.7468	0.7499
	Heterogeneous	**0.7486**	**0.7461**	**0.7469**	**0.7507**
BDL	Symmetric	0.7599	0.7576	0.7576	0.7623
	Homogeneous	0.7481	0.7458	0.7466	0.7498
	Heterogeneous	**0.7481**	**0.7458**	**0.7464**	**0.7500**
Random	Symmetric	0.7774	0.7830	0.7861	0.7856
	Homogeneous	0.7481	0.7458	0.7468	0.7499
	Heterogeneous	**0.7484**	**0.7462**	**0.7471**	**0.7507**

particularly on urban roads. Moreover, the proposed approach has the largest impact on the TPSF topology's fuel efficiency, improving it by 6.5163% and 6.4914% under the Urban Road and Highway Case Study, respectively.

VI. CONCLUSION

A multi-objective asymmetric sliding mode control strategy is proposed in this paper. The asymmetric degrees are incorporated into the control mechanism, causing the topological matrix to change. To obtain the controller's gains, a sliding mode controller incorporating Riccati inequality and Lyapunov analysis is used, ensuring Lyapunov stability and string stability. The NSGA-II algorithm is then used to find the Pareto optimal asymmetric degrees using three platoon performance indices: tracking index, fuel consumption, and acceleration standard deviation.

A platoon of eleven vehicles of different vehicle dynamics is studied. The simulation employs symmetric control, homogeneous asymmetric control, and heterogeneous asymmetric control to demonstrate the superiority of the proposed technique. The Urban Road and Highway Case Study both include 4 topologies, which are the TPSF, PLF, BDL, and Random topology.

The results show that the proposed approach can greatly reduce spacing and velocity errors. The platoon's overall performance improves as stability is achieved. As compared to symmetric control, the proposed heterogeneous asymmetric control improves tracking ability by 60.68% and 76.2%, fuel economy by 0.45% and 3.53%, and driving comfort by 3.52% in the Urban Road and Highway Case Study, respectively. As compared to homogeneous asymmetric control, the proposed approach improves tracking ability while remaining largely unchanged in terms of fuel consumption and driving comfort.

A few questions are to be considered in the future: (i) More essential platoon's evaluation properties should be taken into account. (ii) For the real-time packet losses case, time-varying optimal heterogeneous asymmetric degrees searching could be considered. (iii) Other computationally effective algorithms can be considered for online optimisation.

REFERENCES

[1] Y. Wu, S. E. Li, J. Cortés, and K. Poolla, "Distributed sliding mode control for nonlinear heterogeneous platoon systems with positive definite topologies," *IEEE Trans. Control Syst. Technol.*, vol. 28, no. 4, pp. 1272–1283, Jul. 2020.

[2] Y. Zhu, J. Wu, and H. Su, "V2V-based cooperative control of uncertain, disturbed and constrained nonlinear CAVs platoon," *IEEE Trans. Intell. Transp. Syst.*, vol. 23, no. 3, pp. 1796–1806, Mar. 2022.

[3] Y. Li, C. Tang, S. Peeta, and Y. Wang, "Nonlinear consensus-based connected vehicle platoon control incorporating car-following interactions and heterogeneous time delays," *IEEE Trans. Intell. Transp. Syst.*, vol. 20, no. 6, pp. 2209–2219, Jun. 2019.

[4] H. Guo, J. Liu, Q. Dai, H. Chen, Y. Wang, and W. Zhao, "A distributed adaptive triple-step nonlinear control for a connected automated vehicle platoon with dynamic uncertainty," *IEEE Internet Things J.*, vol. 7, no. 5, pp. 3861–3871, May 2020.

[5] F. Ma, J. Wang, S. Zhu, S. Y. Gelbal, Y. Yang, B. Aksun-Guvenc, and L. Guvenc, "Distributed control of cooperative vehicular platoon with nonideal communication condition," *IEEE Trans. Veh. Technol.*, vol. 69, no. 8, pp. 8207–8220, Aug. 2020.

[6] J. Wang, F. Ma, Y. Yang, J. Nie, B. Aksun-Guvenc, and L. Guvenc, "Adaptive event-triggered platoon control under unreliable communication links," *IEEE Trans. Intell. Transp. Syst.*, vol. 23, no. 3, pp. 1924–1935, Mar. 2022.

[7] H. Li, Z. Chen, B. Fu, Z. Wu, X. Ji, and M. Sun, "Event-triggered vehicle platoon control under random communication noises," *IEEE Access*, vol. 9, pp. 51722–51733, 2021.

[8] Y. Yan, H. Du, Y. Wang, and W. Li, "Multi-objective asymmetric sliding mode control of connected autonomous vehicles," *IEEE Trans. Intell. Transp. Syst.*, early access, Feb. 18, 2022, doi: 10.1109/tits.2022.3149985.

[9] G. Feng, D. Dang, and Y. He, "Robust coordinated control of nonlinear heterogeneous platoon interacted by uncertain topology," *IEEE Trans. Intell. Transp. Syst.*, early access, Dec. 29, 2021, doi: 10.1109/TITS.2020.3045107.

[10] Y. Yan, H. Du, D. He, and W. Li, "A Pareto optimal information flow topology for control of connected autonomous vehicles," *IEEE Trans. Intell. Vehicles*, early access, Jan. 25, 2022, doi: 10.1109/TIV.2022.3145343.

[11] Y. Li, K. Li, T. Zheng, X. Hu, H. Feng, and Y. Li, "Evaluating the performance of vehicular platoon control under different network topologies of initial states," *Phys. A, Stat. Mech. Appl.*, vol. 450, pp. 359–368, May 2016.
[12] Y. Zheng, S. Li, J. Wang, D. Cao, and K. Li, "Stability and scalability of homogeneous vehicular platoon: Study on the influence of information flow topologies," *IEEE Trans. Intell. Transp. Syst.*, vol. 17, no. 1, pp. 14–26, Jan. 2015.
[13] M. J. Musa, S. Sudin, Z. Mohammed, and Y. A. Sha'aban, "Model predictive control for an improved vehicle convoy communication," in *Proc. IEEE 1st Int. Conf. Mechatronics, Automat. Cyber-Phys. Comput. Syst.*, Mar. 2019, pp. 1–6.
[14] O. Orki and S. Arogeti, "Control of mixed platoons consist of automated and manual vehicles," in *Proc. IEEE Int. Conf. Connected Vehicles Expo (ICCVE)*, Nov. 2019, pp. 1–6.
[15] Y. Zheng, S. Li, K. Li, and L.-Y. Wang, "Stability margin improvement of vehicular platoon considering undirected topology and asymmetric control," *IEEE Trans. Control Syst. Technol.*, vol. 24, no. 4, pp. 1253–1265, Jul. 2016.
[16] I. Herman, D. Martinec, Z. Hurák, and M. Sebek, "Harmonic instability of asymmetric bidirectional control of a vehicular platoon," in *Proc. Amer. Control Conf.*, Jun. 2014, pp. 5396–5401.
[17] I. Herman and M. Sebek, "Optimal distributed control with application to asymmetric vehicle platoons," in *Proc. IEEE 55th Conf. Decis. Control (CDC)*, Dec. 2016, pp. 4340–4345.
[18] J. Guo, Y. Luo, and K. Li, "Adaptive fuzzy sliding mode control for coordinated longitudinal and lateral motions of multiple autonomous vehicles in a platoon," *Sci. China Technol. Sci.*, vol. 60, no. 4, pp. 576–586, Dec. 2016.
[19] J.-C. Song and Y.-F. Ju, "Distributed adaptive sliding mode control for vehicle platoon with uncertain driving resistance and actuator saturation," *Complexity*, vol. 2020, pp. 1–12, Jul. 2020.
[20] G. Guo and D. Li, "PMP-based set-point optimization and sliding-mode control of vehicular platoons," *IEEE Trans. Computat. Social Syst.*, vol. 5, no. 2, pp. 553–562, Jun. 2018.
[21] H. Xu and C. Lu, "Design of switched fuzzy adaptive double coupled sliding mode control for vehicles platoon," in *Proc. 5th Int. Conf. Autom., Control Robot. Eng. (CACRE)*, Sep. 2020, pp. 422–426.
[22] Y. Li, C. Tang, S. Peeta, and Y. Wang, "Integral-sliding-mode braking control for a connected vehicle platoon: Theory and application," *IEEE Trans. Ind. Electron.*, vol. 66, no. 6, pp. 4618–4628, Jun. 2019.
[23] D. He, T. Qiu, and R. Luo, "Fuel efficiency-oriented platooning control of connected nonlinear vehicles: A distributed economic MPC approach," *Asian J. Control*, vol. 22, no. 4, pp. 1628–1638, Jul. 2020.
[24] X. T. Yang, K. Huang, Z. Zhang, Z. A. Zhang, and F. Lin, "Eco-driving system for connected automated vehicles: Multi-objective trajectory optimization," *IEEE Trans. Intell. Transp. Syst.*, vol. 22, no. 12, pp. 7837–7849, Dec. 2021.
[25] O. Grodzevich and O. Romanko, "Normalization and other topics in multi-objective optimization," in *Proc. Fields–MITACS Ind. Problems Workshop*, Toronto, ON, Canada, Aug. 2006, p. 89.
[26] G. Yu, P. K. Wong, J. Zhao, X. Mei, C. Lin, and Z. Xie, "Design of an acceleration redistribution cooperative strategy for collision avoidance system based on dynamic weighted multi-objective model predictive controller," *IEEE Trans. Intell. Transp. Syst.*, early access, Jan. 1, 2021, doi: 10.1109/TITS.2020.3045758.
[27] R. Zhao, P. K. Wong, Z. Xie, and J. Zhao, "Real-time weighted multi-objective model predictive controller for adaptive cruise control systems," *Int. J. Automot. Technol.*, vol. 18, no. 2, pp. 279–292, 2017.
[28] Z. Tang, L. Xu, G. Yin, and H. Liu, "L_2 string stability of heterogeneous platoon under disturbances and information delays," in *Proc. Chin. Control Decis. Conf. (CCDC)*, Jun. 2019.
[29] Y. Zheng, S. E. Li, K. Li, and W. Ren, "Platooning of connected vehicles with undirected topologies: Robustness analysis and distributed H-infinity controller synthesis," *IEEE Trans. Intell. Transp. Syst.*, vol. 19, no. 5, pp. 1353–1364, May 2018.
[30] D. F. Coutinho, M. Fu, A. Trofino, and P. Danès, "L_2-gain analysis and control of uncertain nonlinear systems with bounded disturbance inputs," *Int. J. Robust Nonlinear Control*, vol. 18, no. 1, pp. 88–110, Jan. 2008.
[31] S. E. Li, X. Qin, Y. Zheng, J. Wang, K. Li, and H. Zhang, "Distributed platoon control under topologies with complex eigenvalues: Stability analysis and controller synthesis," *IEEE Trans. Control Syst. Technol.*, vol. 27, no. 1, pp. 206–220, Jan. 2019.
[32] H. Rakha, I. Lucic, S. H. Demarchi, J. R. Setti, and M. V. Aerde, "Vehicle dynamics model for predicting maximum truck acceleration levels," *J. Transp. Eng.*, vol. 127, no. 5, pp. 418–425, Oct. 2001.

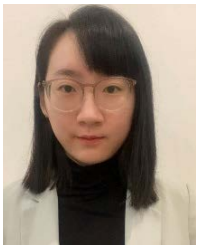

YAN YAN (Student Member, IEEE) received the B.S. degree in mechatronics engineering from the University of Wollongong, Wollongong, Australia, in 2019, where she is currently pursuing the Ph.D. degree with the School of Electrical, Computer and Telecommunications Engineering. Her research interest includes control of connected autonomous vehicles.

HAIPING DU (Senior Member, IEEE) received the Ph.D. degree in mechanical design and theory from Shanghai Jiao Tong University, Shanghai, China, in 2002. He was a Research Fellow with the University of Technology, Sydney, from 2005 to 2009, and a Postdoctoral Research Associate with Imperial College London, from 2004 to 2005, and The University of Hong Kong, from 2002 to 2003. He has been a Professor at the School of Electrical, Computer and Telecommunications Engineering, University of Wollongong, Australia, since 2016.

YAFEI WANG (Member, IEEE) received the Ph.D. degree from the School of Electrical Engineering, The University of Tokyo, Japan, in 2013. He has been an Assistant Professor at the School of Mechanical Engineering, Shanghai Jiao Tong University, China, since 2016.

WEIHUA LI (Senior Member, IEEE) received the Ph.D. degree from Nanyang Technological University (NTU). He was with the School of Mechanical and Aerospace Engineering, NTU, as a Research Associate/Fellow, from 2001 to 2003. He is currently a Senior Professor and the Academic Program Director for Mechatronic Engineering at the University of Wollongong.